ORIGINAL ARTICLE

Carbon Dot-Modified TiO$_2$@SiO$_2$ Aerogel as an Anode for Lithium-Ion Batteries

Zanyu Chen[1] · Jiugang Hu[1] · Kuixing Ding[1] · Jun Tan[1] · Hongshuai Hou[1] · Xiaobo Ji[1]

Abstract

Titanium oxides have been considered promising anode materials for lithium-ion batteries (LIBs). However, the poor conductivity and low specific capacity of bulk titanium oxides limit their application. In this study, a carbon dot-modified TiO$_2$@SiO$_2$ aerogel was successfully fabricated through a facile ambient pressure drying strategy and used as an anode material of LIBs. Benefiting from the crosslinking of carbon dots and the surface modification of SiO$_2$, the as-prepared hierarchical aerogel exhibited a high initial discharge capacity of 974 mAh g^{-1} and maintained a capacity of 299 mAh g^{-1} after 100 cycles at 0.1 A g^{-1}. It also retained a discharge capacity of 111 mAh g^{-1} with a CE of 99.9% at 3 A g^{-1}. The carbon dot-modified cross-linking skeleton contributes to the structural integrity of the TiO$_2$@SiO$_2$ aerogel during repeated insertion/extraction of lithium ions, guaranteeing outstanding cycling and high-rate performance. This ambient pressure drying strategy provides a facile and feasible way to produce high-performance aerogel anode materials for lithium-ion storage.

Highlights

1. Carbon dots-modified TiO$_2$@SiO$_2$ aerogel was fabricated via ambient pressure drying.
2. The hierarchical aerogel shows high initial discharge capacity of 974 mAh g^{-1}.
3. TiO$_2$@SiO$_2$ aerogel exhibits structural integrity and outstanding cycling performance.

1 Introduction

Lithium-ion batteries (LIBs) have been demonstrated to be the most promising energy storage devices for large-scale energy storage, cartable electronic devices, and electrical propulsion applications. Although graphite is commonly used as an anode in commercial LIBs, low theoretical specific capacity limits its further development [1]. In addition, the working potential of graphite is similar to that of lithium metal, thus leading to the formation of parasitic lithium dendrites and short circuits upon overcharging [2]. Therefore, the development of high-performance anode materials for advanced LIBs is urgent.

Titanium oxide is one of the most attractive anode candidate materials due to the safe lithiation potential (~1.7 V vs. Li$^+$/Li), which can effectively avoid lithium dendrite formation [3]. Moreover, the TiO$_2$ anode exhibits only a 3% volume change during the repeated lithiation/delithiation process [4, 5]. However, the poor electron mobility (~10^{-12} S cm^{-1}) and low theoretical specific capacity (~ 177 mAh g^{-1}) limit its practical application [6]. Several strategies have been explored to overcome the aforementioned disadvantages of titanium oxide anodes. The structural design of materials is the most direct way to shorten the ion migration path and improve the Li$^+$ diffusion coefficient. For instance, Kim et al. fabricated hierarchical anatase TiO$_2$ nanoparticles

✉ Jiugang Hu
hujiugang@csu.edu.cn

✉ Jun Tan
csu_tanjun@163.com

1 College of Chemistry and Chemical Engineering, Central South University, Changsha 410083, China

through the hydrolysis of titanium metal–organic framework precursors, the unique porous feature of which enabled the superior rate capability as an anode material for rechargeable LIBs [7]. Zhang et al. designed a unique sandwich-like composite of TiO_2 and carbon nanosheets, which provided abundant active sites for promoting Li-ion migration [8]. In addition, doping with other high-capacity materials is an efficient and facile method to improve the intrinsic property of TiO_2. The SiO_x compound $(0 < x < 2)$ is one of the most valuable and potential doping components due to its extremely high capacity (1000–2000 mAh g^{-1}) [9]. For example, TiO_2/SiO_2 composite fabricated on a Ti foil via the plasma electrical discharge method exhibited high conductivity, a superior discharge capacity of 549 mAh g^{-1} at 100 μA cm^{-2}, and a first cycle Coulombic efficiency (CE) of 56.8% [10]. Zhao et al. reported that the as-prepared Si–TiO_2 composite delivered a high reversible capacity of 1720 mAh g^{-1} over 200 cycles [11]. Although these SiO_x-doped strategies significantly enhanced the specific capacity of TiO_2 composites, the new challenges posed by structure stability cannot be ignored because of the huge volume expansion of Si-based materials [12]. Therefore, new material preparation strategies are still urgently needed for the development of high-stability and high-capacity negative electrodes.

Aerogel is a typical three-dimensional (3D) material with a crosslinked structure and has attracted wide attention in the field of energy storage [13]. Sun et al. found that the Fe_2O_3@ carbonaceous aerogel can promote electrolyte penetration and exhibit better cycling performance than its crystalline powders [14]. Yang et al. prepared a carbon-coated TiO_2 aerogel through the supercritical drying method, which delivered a capacity of 133 mAh g^{-1} at a high current rate of 10 C. The thin and light carbon layer ameliorated the electronic conductivity of Ti-based materials and improved the utilization of the active electrode [15]. Meanwhile, the unique 3D hierarchical structure of aerogels can promote the infiltration of electrolytes and provide loose spaces to buffer structural expansion during the cycling process. In this study, a novel carbon dot-modified TiO_2@SiO_2 aerogel material was fabricated through a facile ambient pressure drying strategy and used as the anode of Li-ion batteries. This preparation strategy not only avoids expensive and dangerous operations in supercritical drying and freeze-drying but also facilitates large-scale applications [16]. The well-dispersed carbon dots can promote the crosslinking of the titanium oxide gel skeleton. Moreover, the silicon oxide coating can promote the stability of the aerogel pore surface and provide an additional capacity contribution. Benefiting from the crosslinking of carbon dots and the surface modification of SiO_2, the obtained aerogel delivers a storage capacity of 299 mAh g^{-1} at 0.1 A g^{-1} after 100 cycles. Even after discharging and charging for 500 cycles, it maintained 62% capacity retention at a high current density of 3 A g^{-1}.

2 Experimental

2.1 Chemicals and Reagents

Tetrabutyl orthotitanate (TBOT) (≥ 99.0%), ethyl alcohol (EtOH) (≥ 99.5%), acetone (≥ 99.0%), N, N-dimethylformamide (≥ 99.8%), and hexane (> 99.0%) were purchased from Aladdin Industrial Corporation. Tetraethyl orthosilicate (TEOS, > 99%), sodium hydroxide, and glacial acetic acid (> 99%) were purchased from Macklin Industrial Corporation.

2.2 Fabrication Procedure of Materials

The aerogel composite precursor was first obtained via a sol–gel process. The carbon dots were prepared according to our previous report [17]. Solution A was obtained by dispersing 5 mL TBOT in 9 mL ethanol to obtain. Glacial acetic acid (1.5 mL) as the pH adjuster was mixed with 9 mL ethanol and 1.5 mL deionized water to obtain solution B. The desired amount of carbon dots and 0.35 mL DMF were added into solution B and stirred for 10 min. Then, the mixed solution was added dropwise into solution A under vigorous stirring. A jelly-like gel was formed after 15 min, which was further cured in an oven of 40 ℃ for 36 h.

In the following three-stage solvent exchange processes, the obtained gel was first immersed with ethanol (9 mL) in an airtight vessel for 24 h to obtain alcogel. After removing the swapped liquid, the obtained alcogel was further soaked in a mixture of TEOS and EtOH (1:2 V/V) for 24 h. After removing the residual liquid, 9 mL hexane was added into the vessel for the third solvent exchange. All of the above solvent exchange processes were operated at 60 ℃. After standing drying at 40 ℃ in a vacuum oven, the aerogel precursor was obtained. The carbon dot-modified TiO_2@SiO_2 aerogel (CTO) can be obtained when the precursor was calcined in an Ar atmosphere at 500 ℃ for 2 h with a heating rate of 3 ℃/min. The samples with different contents of carbon dots (0, 75, and 150 mg) were named CTO-0, CTO-75, and CTO-150, respectively.

Finally, the obtained CTO-150 was further washed with a 2 mol/L NaOH solution to remove the superfluous silicon components and then dried at 60 ℃ for 12 h. The obtained product was named the NCTO aerogel. For comparison, a TiO_2 xerogel was prepared under the same condition without the three-stage solvent exchange process.

2.3 Characterization Methods

The morphologies of the products were determined via scanning electron microscopy (SEM, Quanta 200, FEI Company, Netherlands) and transmission electron microscopy

(TEM, JEM-2100F, JEOL Company, Japan). The specific surface area and pore size of the aerogels were measured via the Brunauer–Emmett–Teller method (BET, ASAP 2020, Micromeritics Co., USA). The crystalline structure was determined via powder X-ray diffraction (XRD, Ultima IV D/max-7500, Rigaku Co., Japan). The carbon content of the CTO and NCTO samples was measured in the air via thermogravimetric analysis (SDT Q600, TA Instruments, USA) from 25 ℃ to 750 ℃ at 10 ℃ /min.

2.4 Electrochemical Measurements

The electrodes were prepared by casting the slurry composed of an active material (80 wt %), Super P (10 wt %), and deionized water (10 wt %) on a copper collector and then drying in a vacuum oven at 60 ℃ for 12 h. The electrochemical performances were assessed using CR2016 coin-type batteries, which consisted of the pure lithium wafer as the cathode. The composition of the electrolyte was 1 mol/L $LiPF_6$ in a mixed solution of ethylene carbonate, dimethyl carbonate, and ethyl methyl carbonate (1:1:1, V/V/V). The prepared electrode was cut into a circular shape of 14 mm diameter and subjected to a battery test. The batteries were assembled in argon and aged for 24 h before the electrochemical measurements. The galvanostatic discharging/ charging tests were performed via a battery test system (LAND, CT2001A) between 0.01 V and 3 V at 25 ± 0.5 ℃. The cyclic voltammetry (CV) tests were performed on a CHI660E electrochemical workstation in the potential range of 0.01–3.0 V.
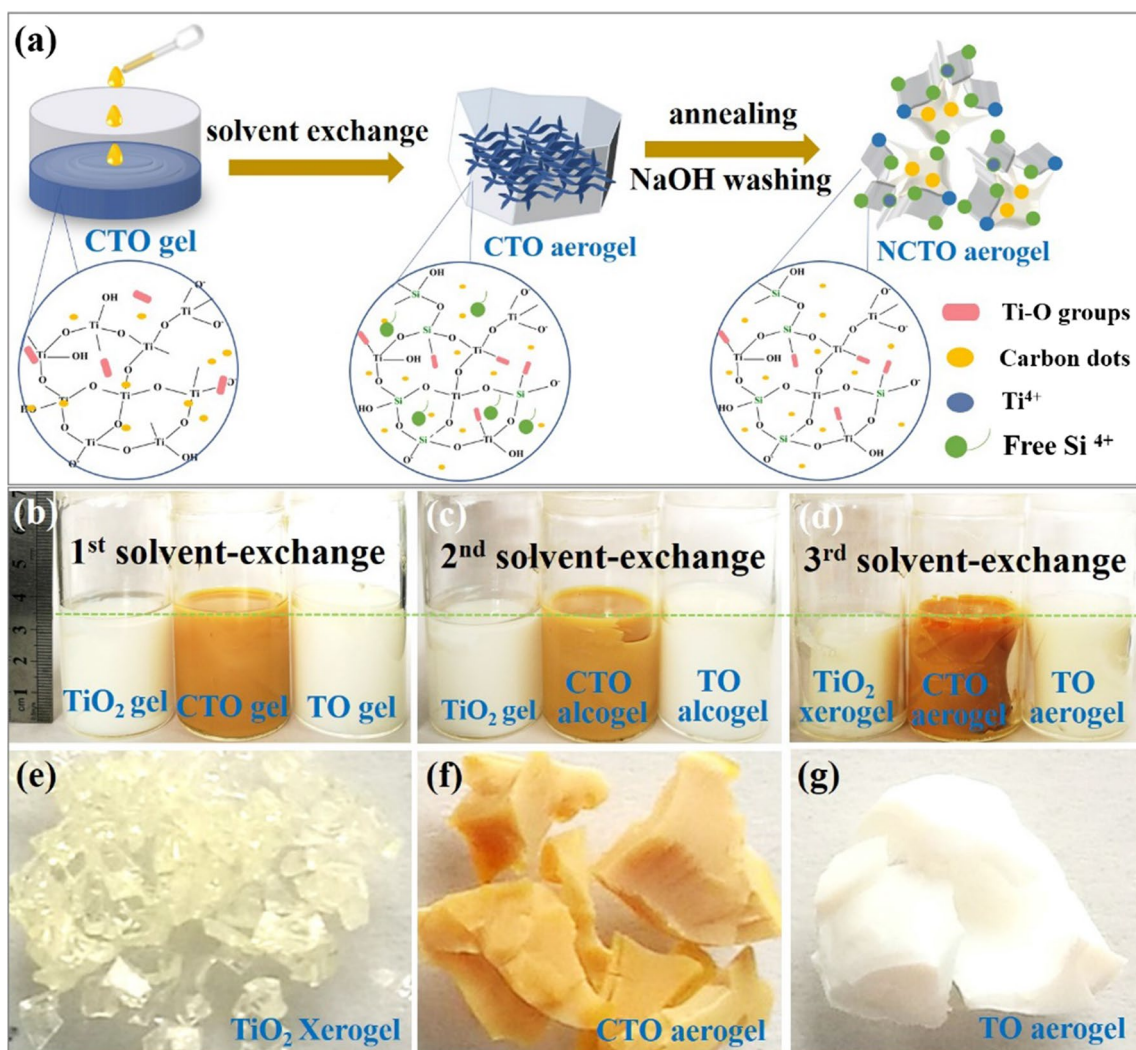

Fig. 1 **a** Schematic illustration of the preparation process of CTO aerogels; **b–d** photographs of the three-stage solvent exchange process; and **e–g** photographs of the TiO_2 xerogel, CTO aerogel, and TO aerogel

3 Results and Discussion

The fabrication process of the aerogels via ambient pressure drying is schematically shown in Fig. 1a, and the corresponding photographs are presented in Figs. 1b–d. TiO_2 gel monoliths were prepared via TBOT hydrolysis polymerization. Carbon dots were introduced into the precursor solution and dispersed sufficiently to form a homogeneous orange–yellow gel. In the three-stage solvent exchange process, the resulting gels were first soaked in an ethanol solution to exchange the free water in the matrix (Fig. 1b). Secondly, the gels were further immersed in a mixed solution of TEOS and ethanol to improve the skeleton network strength (Fig. 1c). Finally, the gels were soaked in an anhydrous *n*-hexane solution to exchange excess TEOS (Fig. 1d). As shown in Figs. 1e–g, the TiO_2 xerogel exhibits a crystalline and translucent feature. Through the three-stage solvent exchange process, the obtained CTO aerogel has loose morphology and larger volume than the TiO_2 xerogel due to the crosslinking of carbon dots and the surface modification of SiO_2. Moreover, it presents an earthy yellow color due to the introduction of carbon dots. The CTO aerogel was further calcined to form a stable aerogel skeleton, which can be used as the anode of LIBs. In comparison, the TiO_2 aerogel (denoted as TO) without carbon dots exhibited light and loose monolith.

The morphologies of the TiO_2 xerogel and aerogels are shown in Fig. 2. In Fig. 2a, the TiO_2 xerogel composite has a smooth surface and nonuniform block structure with a size of 40–100 μm. Compared with the TiO_2 xerogel, the CTO-0 shows a smaller particle size ranging from 15 to 30 μm and a rougher surface because of the three-stage solvent exchange process (Fig. 2b). After adding carbon dots, the surface of the CTO-75 and CTO-150 nanoparticles further became rough (Figs. 2c and d). Interestingly, there are many thin and nonuniform aggregates with sizes smaller than 10 μm on the
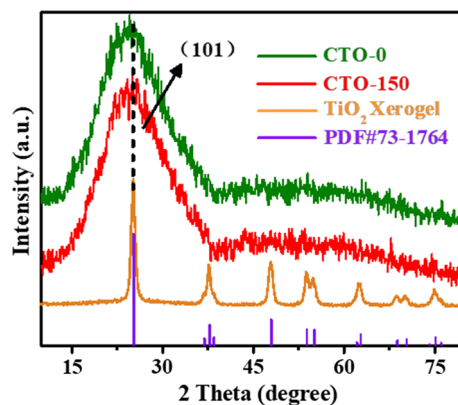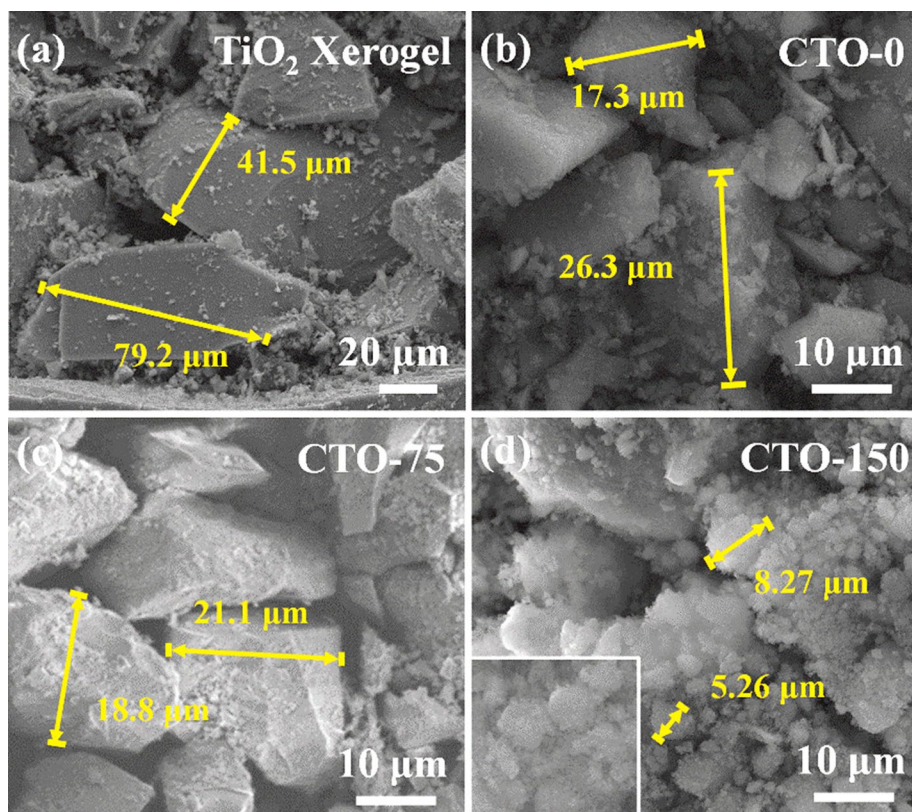

Fig. 3 X-ray diffraction (XRD) patterns of the CTO aerogel and TiO_2 xerogel

Fig. 2 Scanning electron microscopy (SEM) images of **a** the TiO_2 xerogel, **b** CTO-0 aerogel, **c** CTO-75 aerogel, and **d** CTO-150 aerogel

surface of CTO-150 aerogel, which is completely different from the TiO_2 xerogel sample. Carbon dots might be used as chemical additives in the ambient pressure drying process to reduce the stress of capillary pores and enhance the strength of the highly loose aerogel network [18, 19]. In Fig. 3, the TiO_2 xerogel exhibits a good anatase TiO_2 crystallization behavior (PDF#73-1764). However, the CTO aerogel has a more obvious phase change compared to the TiO_2 xerogel, where the wide diffraction peaks indicate the formation of an amorphous TiO_2 aerogel. The wide peak at 20–30° may also confirm the existence of amorphous silicon oxides in

the CTO, which overlaps with the intrinsic characteristic peaks of TiO_2 [20].

To obtain an excellent anode material with high electrochemical activity, the composition and structure of the CTO aerogel composite were optimized. The excess SiO_2 in the aerogel skeleton can be removed through the hydrolysis of Si–O bonds under alkaline conditions [21, 22]. In Fig. 4a, the optimized carbon dot-modified $TiO_2@SiO_2$ aerogel (NCTO) has an irregular particle morphology of 0.7–14 μm and a loose porous surface. In addition, the energy dispersive spectroscopy images confirm that the carbon, titanium,

Fig. 4 **a** Scanning electron microscopy (SEM), **b** elemental mapping, **c** transmission electron microscopy (TEM), and **d** high-resolution TEM images of the NCTO aerogel
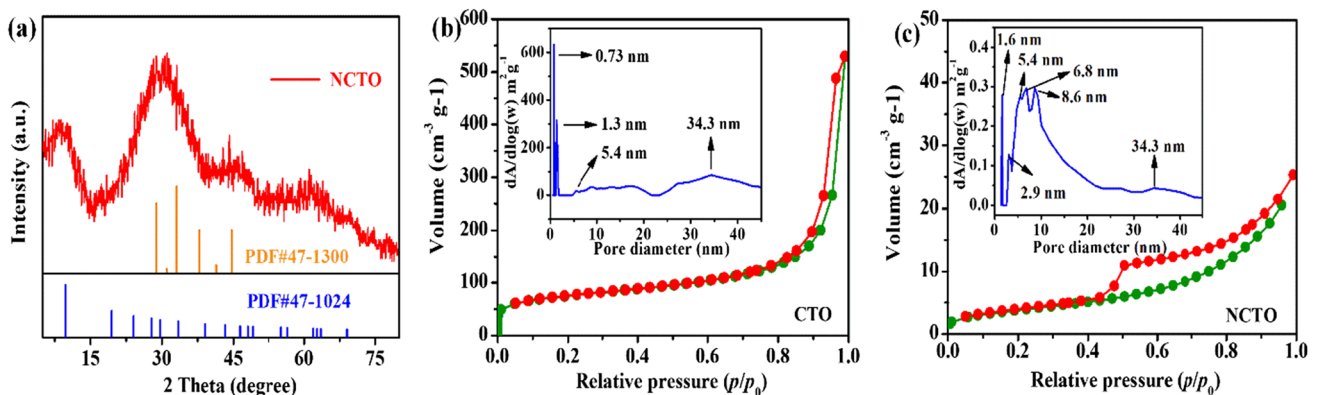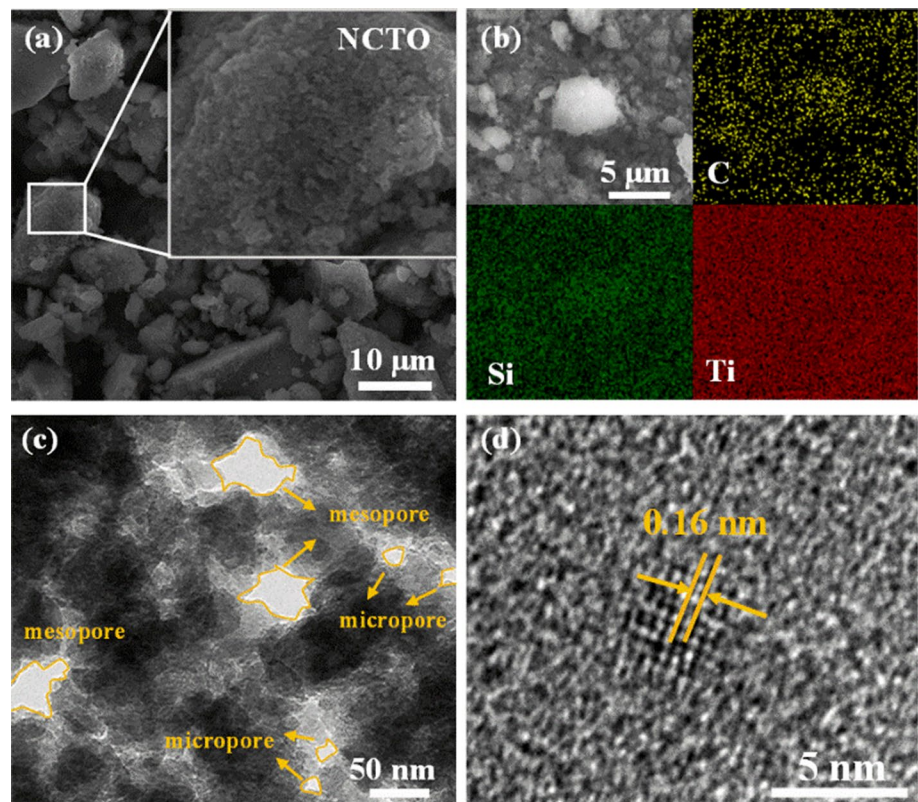

Fig. 5 **a** X-ray diffraction (XRD) pattern of the NCTO aerogel; nitrogen adsorption–desorption isotherm and pore-diameter distribution of the **b** CTO and **c** NCTO aerogels

and silicon elements are homogeneously distributed in the NCTO aerogel, which indicates that the carbon dots and residual silicon oxide components are uniformly dispersed in the titanium oxide aerogel skeleton (Fig. 4b). In Figs. 4c and d, the TEM images confirm the existence of abundant micropores and mesopores in the interior of the NCTO aerogel, potentially providing fast ion transport paths. Moreover, the lattice fringe of 0.16 nm corresponds to the (101) crystal plane of anatase TiO_2 particles.

Compared to the CTO aerogel, the XRD pattern of the NCTO aerogel became slightly sharper (Fig. 5a), indicating the effective exposure of the anatase TiO_2 phase due to the removal of excess SiO_2 (JCPDS No. 47-1300). The diffraction peaks at 9.7, 29.6, 49.2, and 63° can be well indexed to the (201), (600), (220), and (521) planes, respectively, which correspond to the phase characteristics of $H_2Ti_2O_5 \cdot H_2O$ (JCPDS No. 47-1024) [23]. The formation of $H_2Ti_2O_5 \cdot H_2O$ may be attributed to the ion-exchange process of the CTO aerogel in the alkaline medium [24]. The BET analysis shows that the CTO and NCTO aerogels have specific surface areas of 14.03 and 248.89 $m^2 g^{-1}$, respectively. This result indicates that removing the excess SiO_2 can effectively expose the porous structure inside the aerogel. In Figs. 5b and c, the CTO aerogel shows a near-type-I isotherm shape, corresponding to the typical microporous adsorption process [25]. However, the NCTO aerogel exhibits a type IV curve with a type H4 hysteresis loop, indicating the presence of narrow slit-like pores [26]. Based on the Barrett–Joyner–Halenda equation, the NCTO aerogel has abundant pore structures at a range of 0.7–34.3 nm, and the main pore size distribution is 1–10 nm. These results demonstrated that the NaOH washing procedure is beneficial to the formation of the uniform open pore structure and exposure of more active sites. The small pore structure of the NCTO aerogel would provide effective diffusion channels for Li^+ in the charge/discharge process [27].

Figure 6a exhibits the cycling performance of the TiO_2 xerogel and aerogels at 100 mA g^{-1}. The discharge gravimetric capacity of the NCTO aerogel is 310 mAh g^{-1} after 100 cycles, but it is only 174 and 145 mAh g^{-1} for the CTO aerogel and TiO_2 xerogel, respectively. The NCTO and CTO electrodes show higher electrochemical activities than the TiO_2 xerogel due to the presence of a porous structure. Although the CTO aerogel had a high initial discharge capacity of 811 mAh g^{-1}, it exhibited a faster decay process than the other two materials because the excess silicon oxide in CTO would result in volume expansion and structure collapse during the lithium insertion/extraction process [4]. The NCTO aerogel exhibited a high initial discharge capacity of 974 mA h g^{-1} and a CE of 38%, which gradually increased to 95% in the fifth cycle. Figure 6b displays the first four cyclic voltammetry (CVs) curves of the NCTO composite at a scan rate of 0.2 mV s^{-1}. The peak position difference between the first and subsequent scan curves can be observed, which may be related to the irreversible reaction of the silicon oxide component and Li ions [28]. These CV curves are almost identical from the second to the fourth scans, indicating the good reaction reversibility of the titanium oxide aerogel skeleton. The peaks at approximately 1.22 and 2.11 V are attributed to the reaction of titanium oxide [29]. The cathodic peak near 0.2 V was caused by the lithiation process of the silicon oxide component, whereas the anodic peak at 0.52 V was assigned to the transformation process from amorphous $Li_2Si_2O_5$ to SiO_2. Figure 6c shows that several voltage plateaus are consistent with the above results of the CV curves. Moreover, these voltage plateaus barely changed during the 5th to 100th cycles, indicating that the NCTO aerogel has a stable structure during cycling.

In addition, the NCTO aerogel electrode exhibited an outstanding rate capability, with average discharge capacities of 309, 245, 198, 104, 65, and 40 mAh g^{-1} at rates of 0.1, 0.5, 1, 5, 10, and 20 A g^{-1}, respectively. Even after returning to 0.5 A g^{-1}, it still showed a specific discharge capacity of 228 mAh g^{-1}. Therefore, the hierarchical structure of the NCTO aerogel is conducive to high-rate performance. At a high current density of 3 A g^{-1}, the NCTO electrode also retained 111 mAh g^{-1} with a CE of around 99.9% and

Table 1 Comparison of the electrochemical performances of the NCTO and reported titanium-based materials

| Anode	Counter electrodes	Specific capacity		Cycling performance			References
		Current (A g^{-1})	Capacity (mAh g^{-1})	Current (A g^{-1})	Cycle number	Capacity (mAh g^{-1})	
NCTO Composites	Li foil	0.1	309	3	500	111	This work
HNS TiO_2	Li foil	0.1	298	2	300	196	[30]
SNG/TiO_2	Li foil	1	148.8	5	1000	98	[31]
TiO_2/rGO	Li foil	0.1	206	5	200	128	[32]
C@TiO_2 Composites	Li foil	0.1	237	1.6	100	176	[33]
rGO/TiO_2 nanotubes	Li foil	0.1	263	5	100	102	[34]
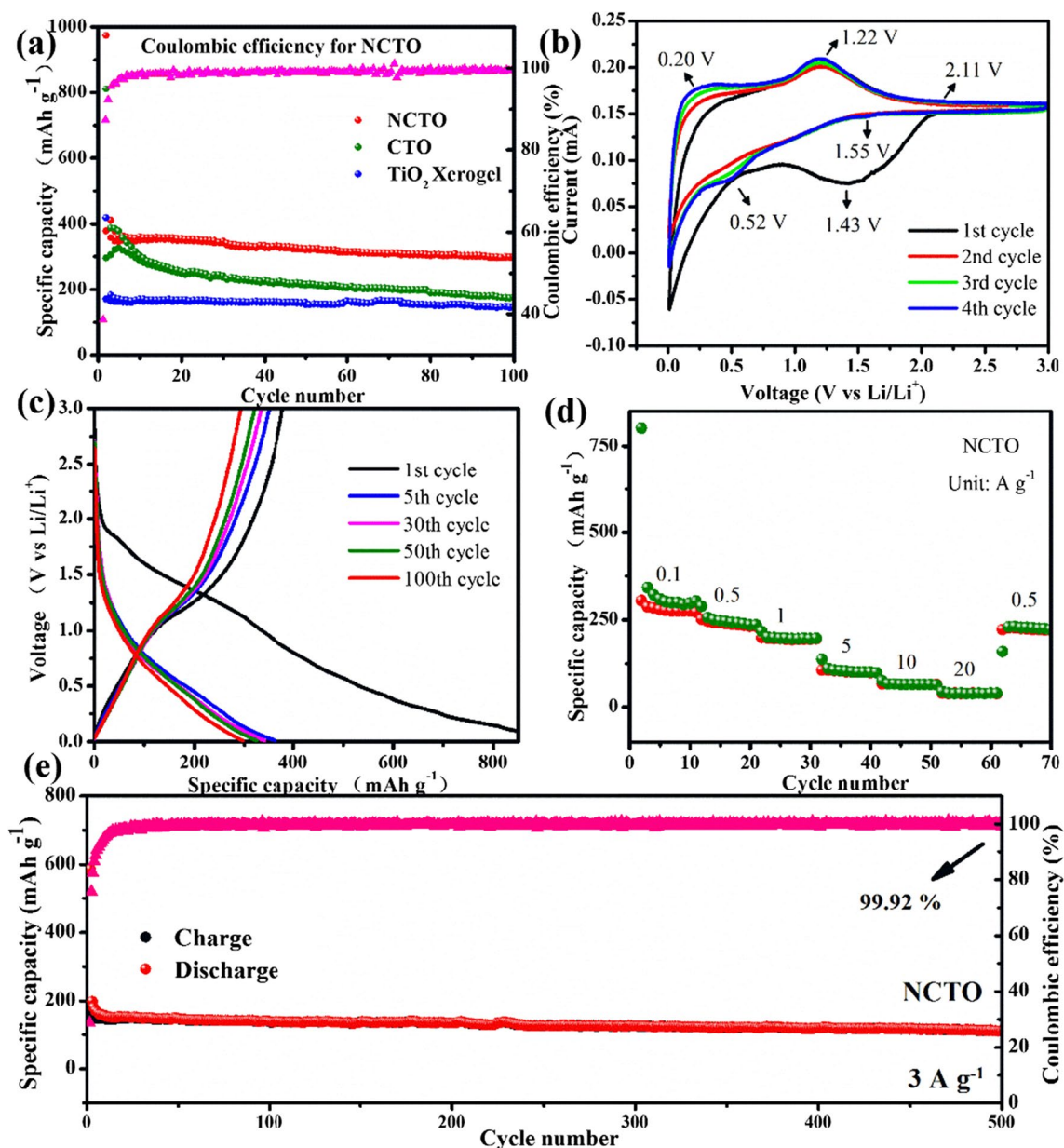
Fig. 6 **a** Cycling performances of the NCTO, CTO, and TiO$_2$ xerogel electrodes at 100 mA g^{-1} and the Coulombic efficiency of the NCTO aerogel; **b** cyclic voltammetry curves, **c** galvanostatic discharge/ charge profiles at 100 mA g^{-1}, **d** rate performance, and **e** long-term cycling performance of the NCTO aerogel at 3 A g^{-1}

still exhibited an excellent capacity retention of 62% after 500 cycles (Fig. 6e). Moreover, the electrochemical performance of the NCTO composite is superior to some reported titanium-based materials, as shown in Table 1. The compositional and cross-linked structure synergistically ensured the high capacity and stability of the TiO$_2$@SiO$_2$ aerogel anode material. In Figs. 7a and b, the thickness of the NCTO electrode can be determined because its surface and cross

section show a significantly different contrast. The active substance still maintained its original thickness without severe collapse even after 100 cycles at 100 mA g^{-1}. These results demonstrate that benefiting from the crosslinking of carbon dots and the surface modification of SiO$_2$, the NCTO electrode keeps its structural integrity during the repeated insertion/extraction of lithium ions and ensures outstanding cycling performance.

Fig. 7 Scanning electron microscopy (SEM) images of the NCTO aerogel anodes **a** before and **b** after 100 cycles at 100 mA g^{-1}
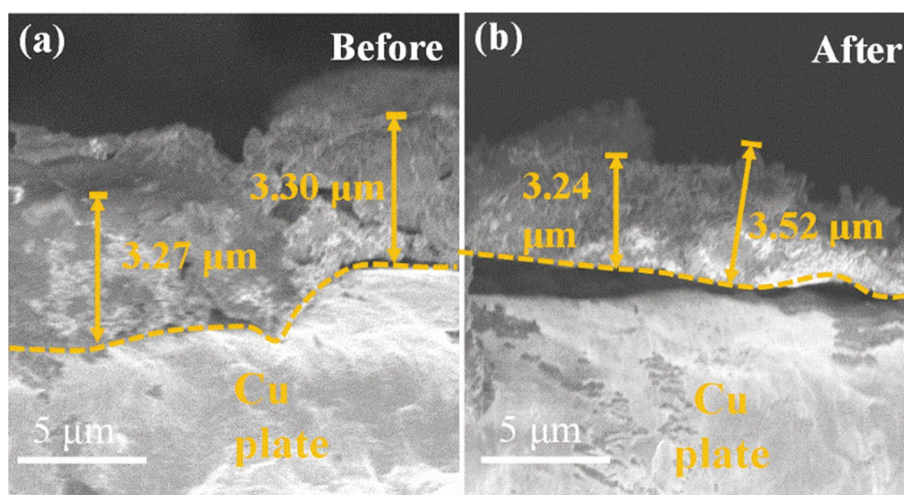
4 Conclusions

In summary, the carbon dot-modified TiO_2@SiO_2 aerogel was fabricated through the ambient pressure drying strategy. Because of the crosslinking of carbon dots and the surface modification of SiO_2, the hierarchical aerogel exhibited a high initial discharge capacity of 974 mAh g^{-1} and remained 299 mAh g^{-1} with a high retention of 80% after 100 cycles at 0.1 A g^{-1}. At a high current density of 3 A g^{-1}, it also retained 111 mAh g^{-1} with a CE of around 99.9% and still exhibited an excellent capacity retention of 62% after 500 cycles. The unique cross-linking and open pore structure of the TiO_2@SiO_2 aerogel can keep the structural integrity for repeated insertion/extraction of lithium ions, guaranteeing outstanding cycling and high-rate performance. The ambient pressure drying strategy can provide a facile and feasible way to produce high-performance aerogel anode materials for lithium-ion storage.

Author Contributions All authors read and approved the final manuscript.

Availability of Data and Materials The datasets generated during and/or analyzed during the current study are available from the corresponding author upon reasonable request.

Declarations

**Competing interests** The authors declare that they have no conflict of interest.

References

1. Jin B, Gao F, Zhu Y-F, Lang X-Y, Han G-F, Gao W, Wen Z, Zhao M, Li J-C, Jiang Q (2016) Facile synthesis of non-graphitizable polypyrrole-derived carbon/carbon nanotubes for lithium-ion batteries. Sci Rep 6:19317

2. Su D, Liu L, Liu Z, Dai J, Wen J, Yang M, Jamil S, Deng H, Cao G, Wang X (2020) Electrospun Ta-doped TiO_2/C nanofibers as a high-capacity and long-cycling anode material for Li-ion and K-ion batteries. J Mater Chem A 8:20666–20676

3. Li Y, Tang X, Zhou X, Li L, Jiang S (2020) Improvement of lithium ion storage in titanium dioxide nanowires by introducing interfacial capacity. Appl Surf Sci 505:144649

4. Babu B, Ullattil SG, Prasannachandran R, Kavil J, Periyat P, Shaijumon MM (2018) Ti^{3+} induced brown TiO_2 nanotubes for high performance sodium-ion hybrid capacitors. ACS Sustain Chem Eng 6:5401–5412

5. Xu J, Jia C, Cao B, Zhang WF (2007) Electrochemical properties of anatase TiO_2 nanotubes as an anode material for lithium-ion batteries. Electrochim Acta 52:8044–8047

6. Ge M, Cao C, Huang J, Li S, Chen Z, Zhang K-Q, Al-Deyab SS, Lai Y (2016) A review of one-dimensional TiO_2 nanostructured materials for environmental and energy applications. J Mater Chem A 4:6772–6801

7. Xiu Z, Alfaruqi MH, Gim J, Song J, Kim S, Thi TV, Duong PT, Baboo JP, Mathew V, Kim J (2015) Hierarchical porous anatase TiO_2 derived from a titanium metal–organic framework as a superior anode material for lithium ion batteries. Chem Commun 51:12274–12277

8. Fu W, Li Y, Chen M-S, Hu Y, Liu B, Zhang K, Zhan C, Zhang M, Shen Z (2020) An orderly arrangement of layered carbon

Nanosheet/TiO2 nanosheet stack with superior artificially interfacial lithium pseudocapacity. J Power Sources 468:228363

9. Liu Z, Yu Q, Zhao Y, He R, Xu M, Feng S, Li S, Zhou L, Mai L (2019) Silicon oxides: a promising family of anode materials for lithium-ion batteries. Chem Soc Rev 48:285–309

10. Wu J, He X, Li G, Deng J, Chen L, Xue W, Li D (2019) Rapid construction of TiO_2/SiO_2 composite film on Ti foil as lithium-ion battery anode by plasma discharge in solution. Appl Phys Lett 114:043903

11. Yang J, Wang Y, Li W, Wang L, Fan Y, Jiang W, Luo W, Wang Y, Kong B, Selomulya C, Liu HK, Dou SX, Zhao D (2017) Amorphous TiO_2 shells: a vital elastic buffering layer on silicon nanoparticles for high-performance and safe lithium storage. Adv Mater 29:1700523

12. Wasalathilake KC, Hapuarachchi SNS, Zhao Y, Fernando JFS, Chen H, Nerkar JY, Golberg D, Zhang S, Yan C (2020) Unveiling the working mechanism of graphene bubble film/silicon composite anodes in Li-ion batteries: from experiment to modeling. ACS Appl Energy Mater 3:521–531

13. He J, Yang JG, Jiang J, Xu MW, Wang Q (2021) Constructing reduced graphene oxide network aerogel supported TiO_2(B) (Bronze phase TiO_2) as anode material for lithium-ion storage. J Alloy Compd 853:157330

14. Huang Y, Lin Z, Zheng M, Wang T, Yang J, Yuan F, Lu X, Liu L, Sun D (2016) Amorphous Fe_2O_3 nanoshells coated on carbonized bacterial cellulose nanofibers as a flexible anode for high-performance lithium ion batteries. J Power Sources 307:649–656

15. Zhang C, Liu S, Qi Y, Cui F, Yang X (2018) Conformal carbon coated TiO_2 aerogel as superior anode for lithium-ion batteries. Chem Eng J 351:825–831

16. Du D, Jiang Y, Feng J, Li L, Feng J (2020) Facile synthesis of silica aerogel composites via ambient-pressure drying without surface modification or solvent exchange. Vacuum 173:109117

17. Hou HS, Banks CE, Jing MJ, Zhang Y, Ji XB (2015) Carbon quantum dots and their derivative 3D porous carbon frameworks for sodium-ion batteries with ultralong cycle life. Adv Mater 27:7861–7866

18. Zhang L, Lei Y, He P, Wu H, Guo L, Wei G (2022) Carbon material-based aerogels for gas adsorption: fabrication, structure design, functional tailoring, and applications. Nanomaterials 12(18):3172

19. Nah H-Y, Parale VG, Jung H-N-R, Lee K-Y, Lim C-H, Ku YS, Park H-H (2018) Role of oxalic acid in structural formation of sodium silicate-based silica aerogel by ambient pressure drying. J Sol-Gel Sci Technol 85:302–310

20. Meng XL, Huo HY, Cui ZH, Guo XX, Dong SM (2018) Influences of oxygen content on the electrochemical performance of a-SiO_x thin-film anodes. Electrochim Acta 283:183–189

21. Okunev AG, Shmakov AN, Danilyuk AF, Aristov YI (2000) Fragmentation of SiO_2 aerogels in aqueous NaOH solutions studied in situ by SAXS using SR. Nucl Instrum Methods Phys Res Sect A 448:261–266

22. Okunev AG, Shaurman SA, Danilyuk AF, Aristov YI, Bergeret G, Renouprez A (1999) Kinetics of the SiO_2 aerogel dissolution in aqueous NaOH solutions: experiment and model. J Non-Cryst Solids 260:21–30

23. Liu QN, Liu Y, Lei T, Tan YN, Wu H, Li JB (2015) Preparation and characterization of nanostructured titanate bioceramic coating by anodization-hydrothermal method. Appl Surf Sci 328:279–286

24. Yao L, He J, Li T, Ren T (2016) Novel $SiO_2/H_2Ti_2O_5 \cdot H_2O$-nanochain composite with high UV–visible photocatalytic activity for supertransparent multifunctional thin films. Langmuir 32:13611–13619

25. Geng P, Cao S, Guo X, Ding J, Zhang S, Zheng M, Pang H (2019) Polypyrrole coated hollow metal-organic framework composites for lithium-sulfur batteries. J Mater Chem A 7:19465–19470

26. Casula MF, Corrias A, Paschina G (2001) Iron oxide-silica aerogel and xerogel nanocomposite materials. J Non-Cryst Solids 293–295:25–31

27. Liu L, Fan Q, Sun C, Gu X, Li H, Gao F, Chen Y, Dong L (2013) Synthesis of sandwich-like TiO_2@C composite hollow spheres with high rate capability and stability for lithium-ion batteries. J Power Sources 221:141–148

28. Zhang L, Gu X, Yan C, Zhang S, Li L, Jin Y, Zhao S, Wang H, Zhao X (2018) Titanosilicate derived SiO_2/TiO_2@C nanosheets with highly distributed TiO_2 nanoparticles in SiO_2 matrix as robust lithium ion battery anode. ACS Appl Mater Interfaces 10:44463–44471

29. Wang QF, Wang ML, Miao J, Bi WY, Yang H, Zhang M (2019) Fabrication of SiO_2 aerogel supported C/TiO_2 nanocomposite and Li^+ storage performance. J Mater Sci: Mater Electron 30:14834–14846

30. Ding M, Cao L, Miao X, Sang T, Zhang C, Ping Y (2021) Fabrication of hollow TiO_2 nanospheres for high-capacity and long-life lithium storage. Ionics 27:3365–3372

31. Huo J, Ren Y, Xue Y, Liu Y, Guo S (2021) Sulfur/nitrogen dual-doped three-dimensional reduced graphene oxide modified with mesoporous TiO_2 nanoparticles for promising lithium-ion battery anodes. J Alloy Compd 868:159183

32. Yang S, Cao C, Huang P, Peng L, Sun Y, Wei F, Song W (2015) Sandwich-like porous TiO_2/reduced graphene oxide (rGO) for high-performance lithium-ion batteries. J Mater Chem A 3:8701–8705

33. Ren Y, Zhang G, Huo J, Li J, Liu Y, Guo S (2022) Flower-like TiO_2 hollow microspheres with mixed-phases for high-pseudocapacitive lithium storage. J Alloy Compd 902:163730

34. Chen J, Li Y, Mu J, Zhang Y, Yu Z, Han K, Zhang L (2018) C@TiO_2 nanocomposites with impressive electrochemical performances as anode material for lithium-ion batteries. J Alloy Compd 742:828–834
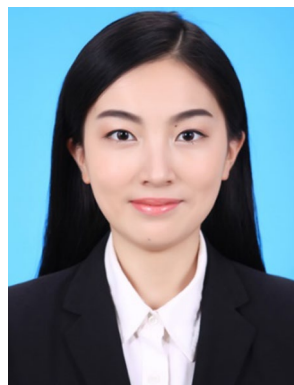
Zanyu Chen received his master's degree in chemistry from Central South University in 2021. Her current research interests are the preparation and application of new energy materials. She has published 4 SCI papers.

Jiugang Hu is an associate professor at College of Chemistry and Chemical Engineering, Central South University. His current research is specializing in efficient recovery and materialization of non-traditional non-ferrous metal resources. He has published more than 70 SCI papers, 9 authorized patents and 1 monograph.

Hongshuai Hou is a professor at College of Chemistry and Chemical Engineering, Central South University. He received Ph.D. at Central South University in 2016. His current research interests are carbon dots materials and key materials for electrochemical energy storage devices. He has published more than 100 papers.

Kuixing Ding received his doctoral degree from Central South University in 2022. Currently, His current research is specializing in non-precious metal catalysts in Zinc-air batteries. He has published 6 SCI papers.

Xiaobo Ji is "Sheng hua" Professor, acts as associate dean in the Department of Chemistry and Chemical Engineering at Central South University. He received Dphil under the supervision of Prof. Richard G. Compton at University of Oxford at 2007, and undertook post-doctor work at MIT with Prof. Donald Sadoway. His current research is specializing in the research & development of battery and Supercapacitor materials and their systems. He has published more than 270 peer-reviewed papers. He is Associate Editor for Electrochemistry Communications.

Jun Tan is an associate professor at College of Chemistry and Chemical Engineering, Central South University. Her current research is specializing in solid waste treatment and preparation of new energy materials.